Electronic Supplementary Material (ESI) for Journal of Materials Chemistry C.


# High-Performance Shortwave Deep-UV Response-Enhanced Photodetector Based on Nanoporous AlGaO/AlGaN with Efficient Light-Harvesting

**Zhihua Zheng [a,b], Yongming Zhao [a], Pengcheng Jian [a], Shizhou Tan [a], Feng Wu [a,*], Weijie Liu [a], Yiming Yang [a], Munho Kim [b], Jiangnan Dai [a,*], Changqing Chen[a]**

[a] Wuhan National Laboratory for Optoelectronics, Huazhong University of Science and Technology, Wuhan 430074, China.

[b] School of Electrical and Electronic Engineering, Nanyang Technological University, Singapore 639798, Singapore.

*Corresponding authors. E-mail addresses: wufeng123@hust.edu.cn (F. Wu), daijiangnan@hust.edu.cn (J. Dai)

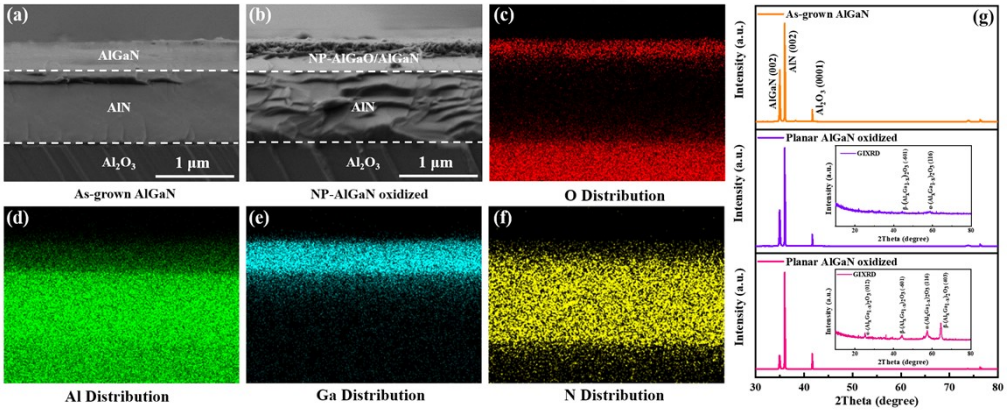


**Fig. S1.** (a) Cross-sectional morphology of the As-grown AlGaN. (b) Cross-sectional morphology, (c) O element, (d) Al element, (e) Ga element and (f) N element distribution of the NP-AlGaN oxidized. (g) XRD ω-2θ patterns for as-grown AlGaN. XRD ω-2θ patterns with the inset of the grazing incident angle XRD patterns for the planar AlGaN oxidized and the NP-AlGaN oxidized.

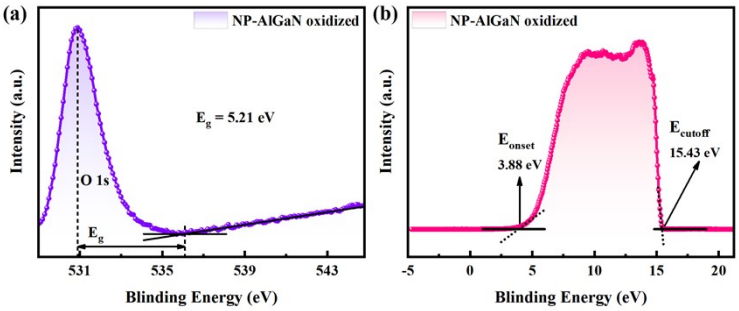


**Fig. S2.** (a) O 1s energy loss spectrum for determining bandgap and (b) UPS spectrum of the NP-AlGaN after oxidation.

The bandgap of the top AlGaO layer in the oxidized NP-AlGaN was extracted by the energy loss spectra of O 1s as illustrated in Fig. S2a. The maximum energy of O 1s peak was set to zero loss energy, followed by the linearly extrapolated the

maximum negative slope of the spectral line to the background level. Then the energy difference between the peak and the intersection provides the bandgap value, demonstrating it of 5.21 eV. In addition, the UPS spectra of the top AlGaO layer in the oxidized NP-AlGaN have been investigated with a monochromatic He I light source (21.22 eV), as shown in Fig. S2b. Similarly, the energy separation ($E_{onset}$) between the Fermi level and the top of valence-band energy was extracted to be 3.88 eV, and the binding energy of the cutoff edge ($E_{cutoff}$) was extracted to be 15.43 eV, which were utilized to deduce the height of the valence band.

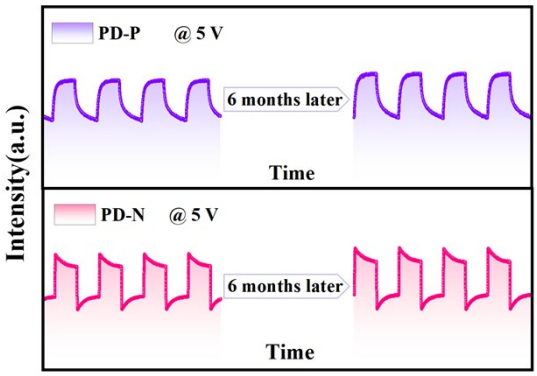


**Figure S3.** Time-dependent photoresponse curves of PD-P and PD-N measured at as-prepared and after 6 months of storage in the ambient air.

**Table S1.** Comparison of the performance parameters of the reported UV PDs based on various nanostructures and planar structures

| Structures | Responsivity (A/W) | Detectivity (Jones) | Response time ($\tau_r/\tau_d$) | $I_{Photo}$-$P_\lambda$ exponent α | PDCR | GBP | Ref. |
|---|---|---|---|---|---|---|---|
| AlGaN nanowires | 0.049 (0 V @254 nm) | - | 83/19 ms | < 1 | - | 2.53 | 47[1] |
| AlGaN APD | 0.13 (20 V @276 nm) | $1.4\times10^{14}$ | - | - | ~ $1\times10^{4}$ | > 1560 | 48[2] |
| AlGaO nanowires | 0.726 (5 V @242 nm) | - | - | - | $1\times10^{3}$ | - | 49[3] |
| β-$Ga_2O_3$ film | 26.1 (10 V @255 nm) | $1.2\times10^{13}$ | 48/18 ms | - | $10^{4}$ | 145 | 50[4] |
| β-$Ga_2O_3$ nanosheets | 3.3 (10 V @254 nm) | $4.0\times10^{12}$ | 30/60 ms | 1.8 | 4.5 | 55 | 51[5] |
| α-$Ga_2O_3$ nanorod | 1.73 (1 V @254 nm) | $2.53\times10^{12}$ | 0.678/0.178 s | 0.78 | $3.79\times10^{4}$ | 9.7 | 52[6] |
| NP- $Ga_2O_3$/GaN | 0.44 (0 V @254 nm) | $2.7\times10^{11}$ | 0.12/0.44 s | - | 272 | 3.7 | 53[7] |
| β-$Ga_2O_3$/NP-GaN | $4.5\times10^{5}$ (10 V @360 nm) | $8.27\times10^{15}$ | 1.09/0.79 s | - | ~ $10^{2}$ | $4.1\times10^{5}$ | 54[8] |
| Mesoporous GaN | ~ $1.4\times10^{4}$ (0.8 V @352 nm) | $5.3\times10^{14}$ | > 20/60 s | 0.2 | - | < 700 | 55[9] |
| NP-GaN nanocolumn/ nanowall network | 7.25-27.72 (2V) | 1.15-1.96× $10^{11}$ | > 10 s | - | ~ 1.5 | - | 56[10] |
| NP-AlGaO/AlGaN | 1.54 (5V @245 nm) | $1.5\times10^{13}$ | 6/7 μs | 0.98 | 6.8× $10^{4}$ | $2.6\times10^{5}$ | This work |

## References


1 D. Wang, C. Huang, X. Liu, H. Zhang, H. Yu, S. Fang, B. S. Ooi, Z. Mi, J. He and H. Sun, *Adv. Opt. Mater.*, 2021, **9**, 2000893.

2 T. Tut, M. Gokkavas, A. Inal and E. Ozbay, *Appl. Phys. Lett.*, 2007, **9**, 163506.

3 X. Zhang, T. He, W. Tang, Y. Ma, X. Wei, D. Wang, H. Zhang, H. Sun, Y. Fan, Y. Cai and B. Zhang, *J. Phys. D. Appl. Phys.*, 2020, **53**, 495105.

4 D. Zhang, W. Zheng, R. C. Lin, T. T. Li, Z. J. Zhang and F. Huang, *J. Alloys Compd.*, 2018, **735**, 150-154.

5 W. Feng, X. Wang, J. Zhang, L. Wang, W. Zheng, P. Hu, W. Cao and B. Yang, *J. Mater. Chem. C*, 2014, **2**, 3254-3259.

6 J. Y. Wei, L. P. Shen, Z. C. Zheng, Y. C. Xu, H. Wu, H. Zhou and H. Wang, *Ceram. Int.*, 2022, 1-6.

7 T. Chen, X. Zhang, Y. Ma, T. He, X. Wei, W. Tang, W. Tang, X. Zhou, H. Fu, L. Zhang, K. Xu, C. Zeng, Y. Fan, Y. Cai and B. Zhang, *Adv. Photonics Res.*, 2021, **2**, 2100049.

8 R. Meng, X. Ji, Z. Lou, J. Yang, Y. Zhang, Z. Zhang, W. Bi, J. Wang and T. Wei, *Opt. Lett.*, 2019, **44**, 2197.

9 L. Liu, C. Yang, A. Patanè, Z. Yu, F. Yan, K. Wang, H. Lu, J. Li and L. Zhao, *Nanoscale*, 2017, **9**, 8142-8148.

10 C. Ramesh, P. Tyagi, B. Bhattacharyya, S. Husale, K. K. Maurya, M. S. Kumar and S. S. Kushvaha, *J. Alloys Compd.*, 2019, **770**, 572-581.